

Quasi-Isentropic Compression of Vapor-Deposited HNAB – Experiments and Analysis

Quasi-Isentropic Compression of Vapor-Deposited HNAB – Experiments and Analysis

C. D. Yarrington, A. S. Tappan, P. E. Specht, and R. Knepper

20th Biennial Conference of the APS Topical Group on
Shock Compression of Condensed Matter,
St. Louis, Missouri, July 9 – 14, 2017.



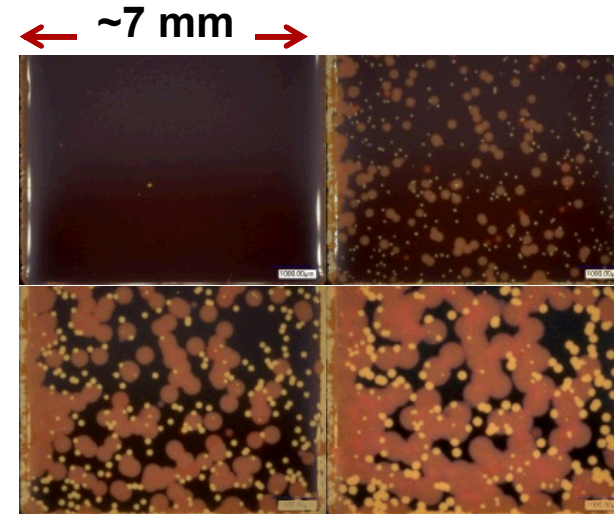
Sandia National Laboratories is a multimission laboratory managed and operated by National Technology and Engineering Solutions of Sandia, LLC., a wholly owned subsidiary of Honeywell International, Inc., for the U.S. Department of Energy's National Nuclear Security Administration under contract DE-NA0003525 SAND2017-xxxx.

HNAB explosive films

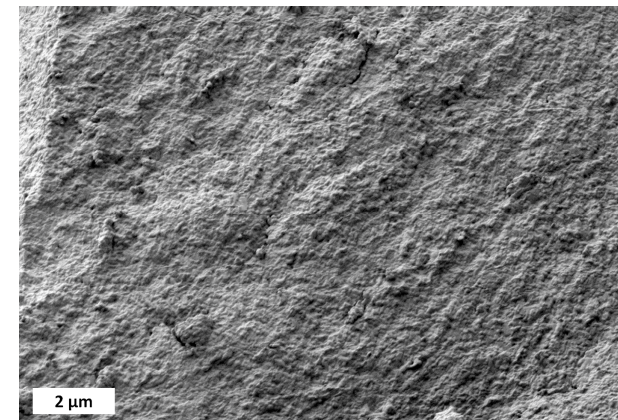
- Vapor-deposited hexanitroazobenzene (HNAB)
- Amorphous (as deposited) then crystallizes (days to weeks)
- Final films are principally HNAB-II, isotropic, nanocrystalline, and >99.5% dense

Knepper, R., Browning, K., Wixom, R.R., Tappan, A.S., Rodriguez, M.A., and Alam, M.K., "Microstructure Evolution during Crystallization of Vapor-Deposited Hexanitroazobenzene Films," *Propellants, Explosives, Pyrotechnics*, vol. 37, pp. 459 – 467, 2012.

Tappan, A.S., Wixom, R.R., and Knepper, R., "Geometry effects on detonation in vapor-deposited hexanitroazobenzene (HNAB)," *AIP Conference Proceedings*, vol. 1793, no. 1, p. 030036, 2017/01/13, 2015.



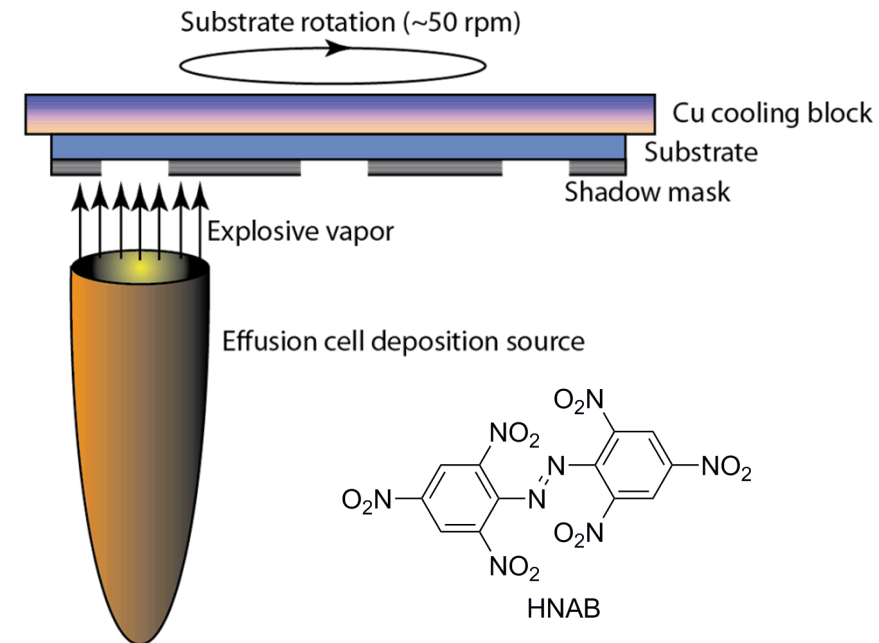
HNAB crystallization, time-lapse
65 °C, 24 min./image.



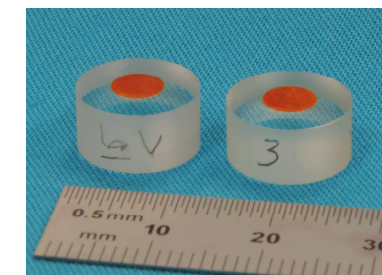
Fracture cross-section micrograph
of 35 °C crystallized HNAB.

HNAB physical vapor deposition

- Vacuum thermal evaporation
- Cooled substrate holder
- 0.2 to 0.3 μm Al reflector
- 189 and 169 μm HNAB
- Crystallization of amorphous HNAB nucleated by gentle roughening



Optical micrographs of HNAB after deposition (left), after roughening (middle) and after crystallization.



HNAB films on PMMA and LiF.

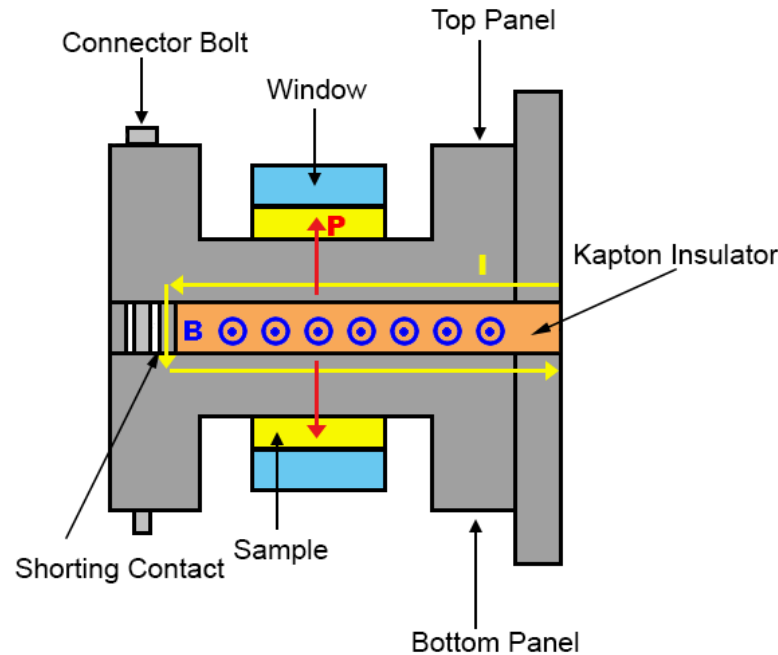
Quasi-Isentropic Compression

- A continuous measurement of the HNAB quasi-isentrope was obtained through magnetic ramp compression
 - Quasi-isentropic because not completely reversible
- Current flow generates a magnetic field between the top and bottom panels

- The resulting Lorenz force, $\mathbf{P} = \mathbf{I} \times \mathbf{B}$, compresses the sample [1]

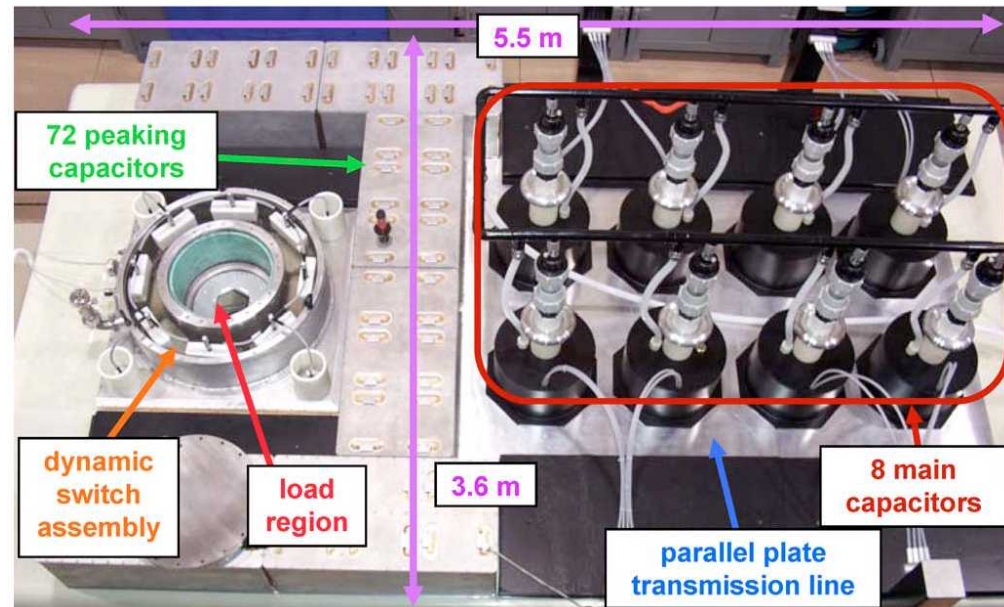
$$P = k_e \frac{B^2}{2\mu} = k_e \frac{\mu}{2} \left(\frac{I}{w} \right)^2$$

- Experiments performed on the VELOCE Pulsed Power Machine [1] at Sandia National Laboratories



VELOCE Pulsed Power Machine

- VELOCE [1] is a compact pulsed power machine located at the Dynamic Integrated Compression Experimental (DICE) facility at Sandia National Laboratories
 - 3 MA of current
 - Rise times from 440 to 550 ns
 - Pressures from 5 -20 GPa

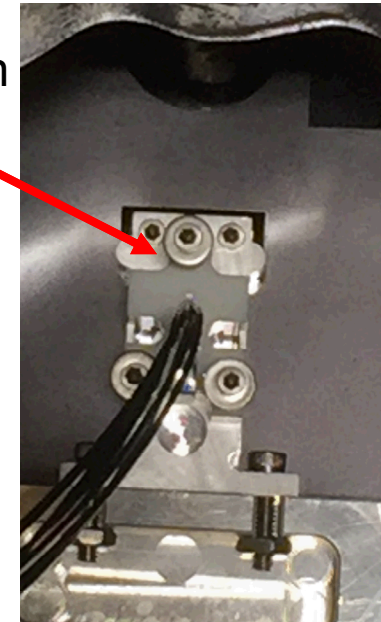


From T. Ao et al., Rev. Sci. Instrum. **79**, 013903 (2008).

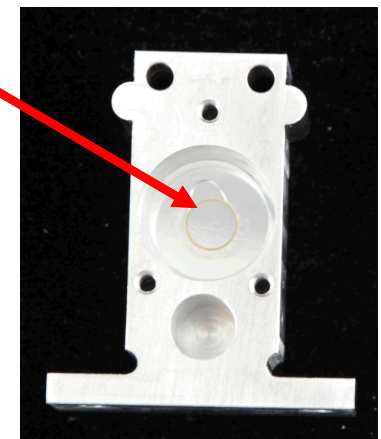
Experimental Parameters

- Al 6061 panels with a 1.5 mm floor thickness
- Samples were bonded to the panel with **Sylgard® 527** silicone and secured with a compression system
- Velocity records were recorded with both VISAR and PDV

Compression System



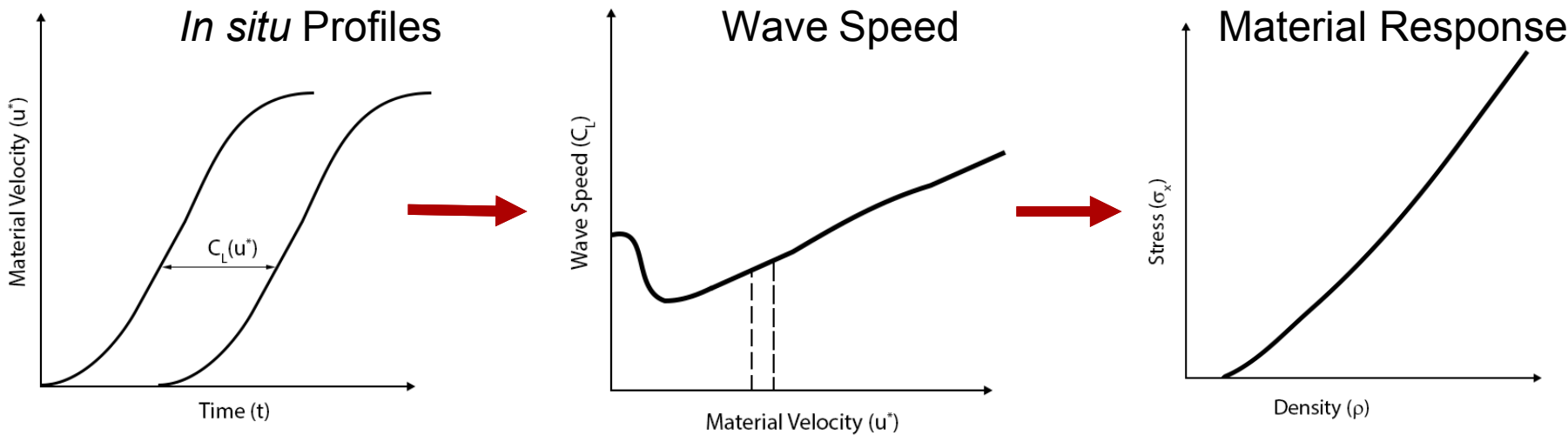
HNAB-II



Experiment	HNAB Thickness	Window	Current	Rise Time
1	169 μm	LiF	1.9 MA	493 ns
2	189 μm	PMMA	2.1 MA	504 ns

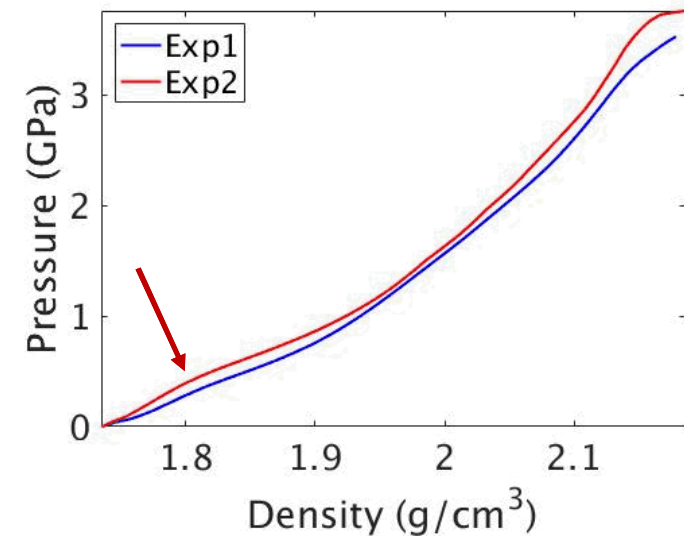
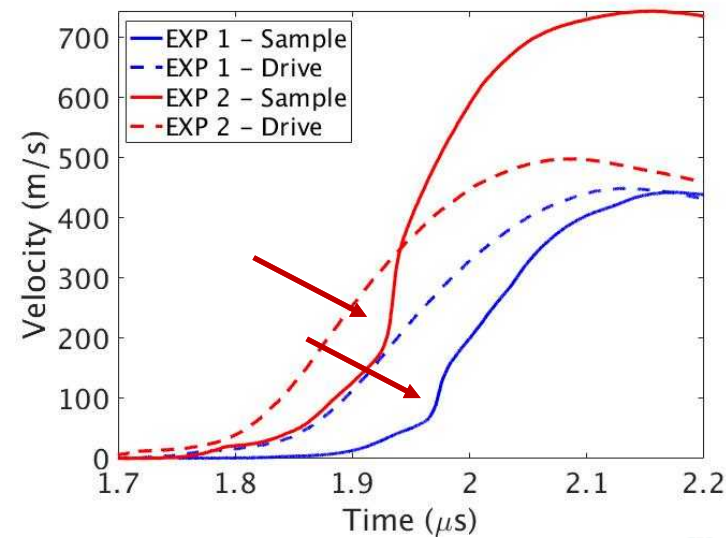
Quasi-Isentrope Determination

- Quasi-isentrope is determined with Lagrangian, or *in situ*, material velocities at two locations in the sample [2]
 - Direct Lagrangian analysis
 - $dv = -\frac{-du^*}{\rho_0 C_L(u^*)}$ $d\sigma_x = \rho_0 C_L(u^*) du^*$
- Usually velocimetry measurements are at window interfaces and must be mapped to *in situ* velocities
 - Inverse Lagrangian analysis (ILA) [2]



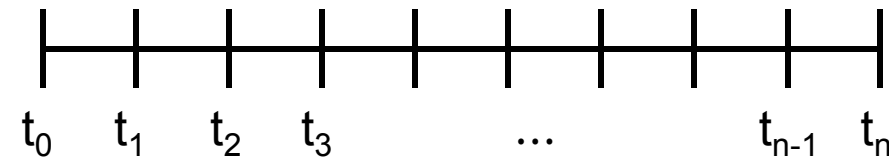
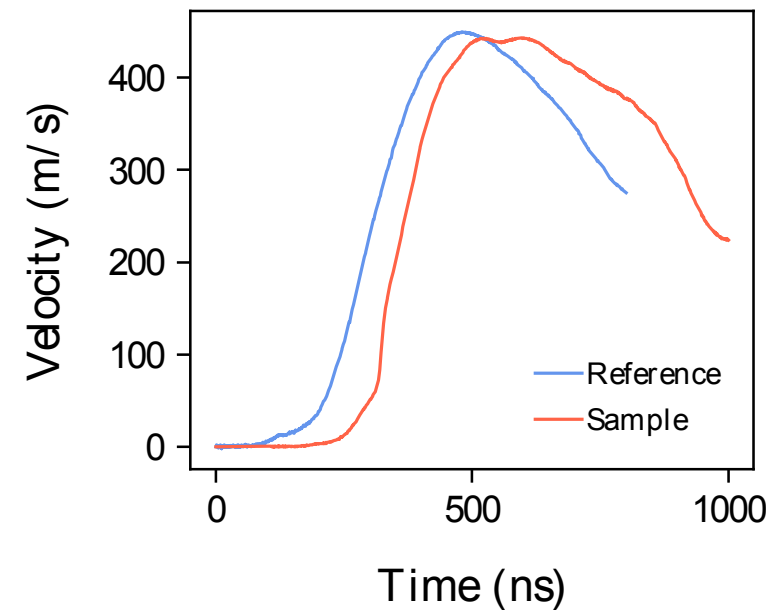
Experimental Results

- Interface velocity records from each experiment indicated a low pressure (~ 0.6 GPa) phase change in HNAB-II
- Phase transition cast doubt on the obtained quasi-isentrope
 - Invalidates the isentropic flow assumptions underlying the analysis method
 - Current efforts are underway to perform ILA through phase transitions



EOS – Alternate Determination Methods

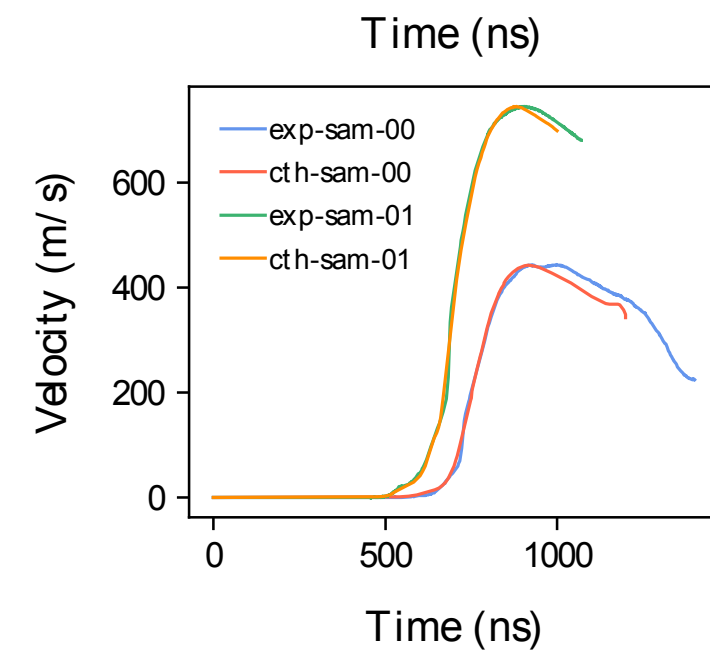
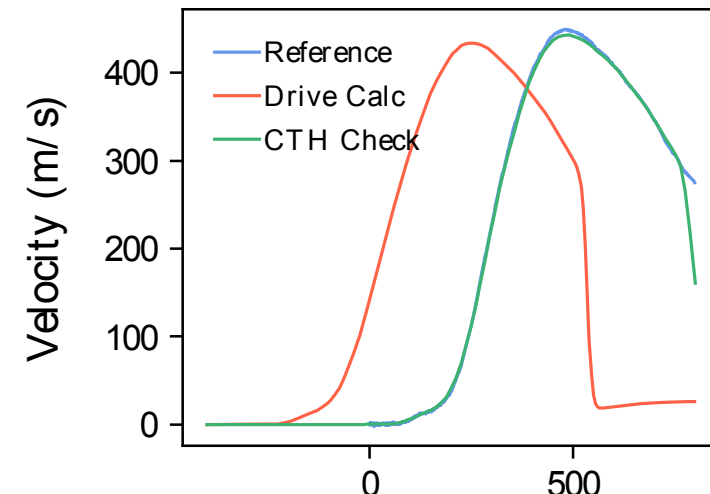
- Backward integration technique (Hayes, 2001)
 - Time partitioned
 - Equations of motion marched backwards in space
 - Visar record is initial condition
 - Must know material response of reference material
- Each veoce shot has sample side (HNAB-II) and reference side (1100-Al) that are subjected to the same drive conditions



Each iteration takes the solution back dx , until the drive surface is reached

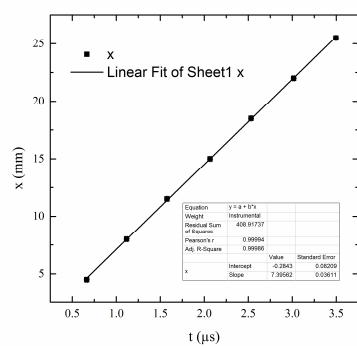
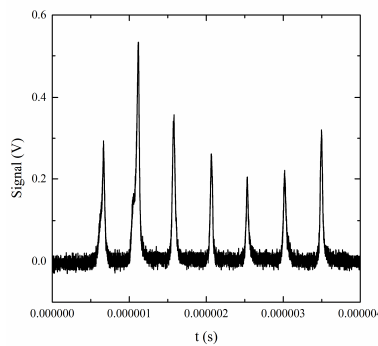
Drive Verification and EOS determination

- The drive conditions are verified by running a standard forward calculation using the drive stress history
- Sample geometry run in a forward calculation with unknown EOS and constitutive model
- DAKOTA is used to optimize Mie-Gruneisen and EPPVM constitutive model parameters

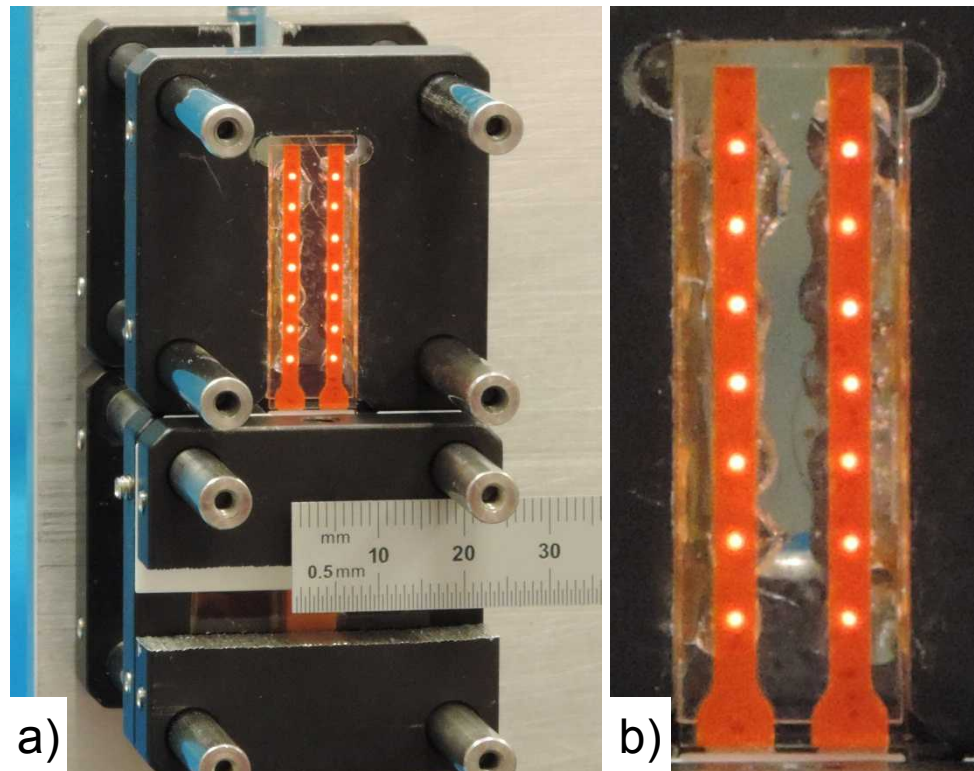


Critical detonation thickness experiment

- Two experiments (HNAB lines) each shot
- Optical fibers deliver detonation light to photodetector



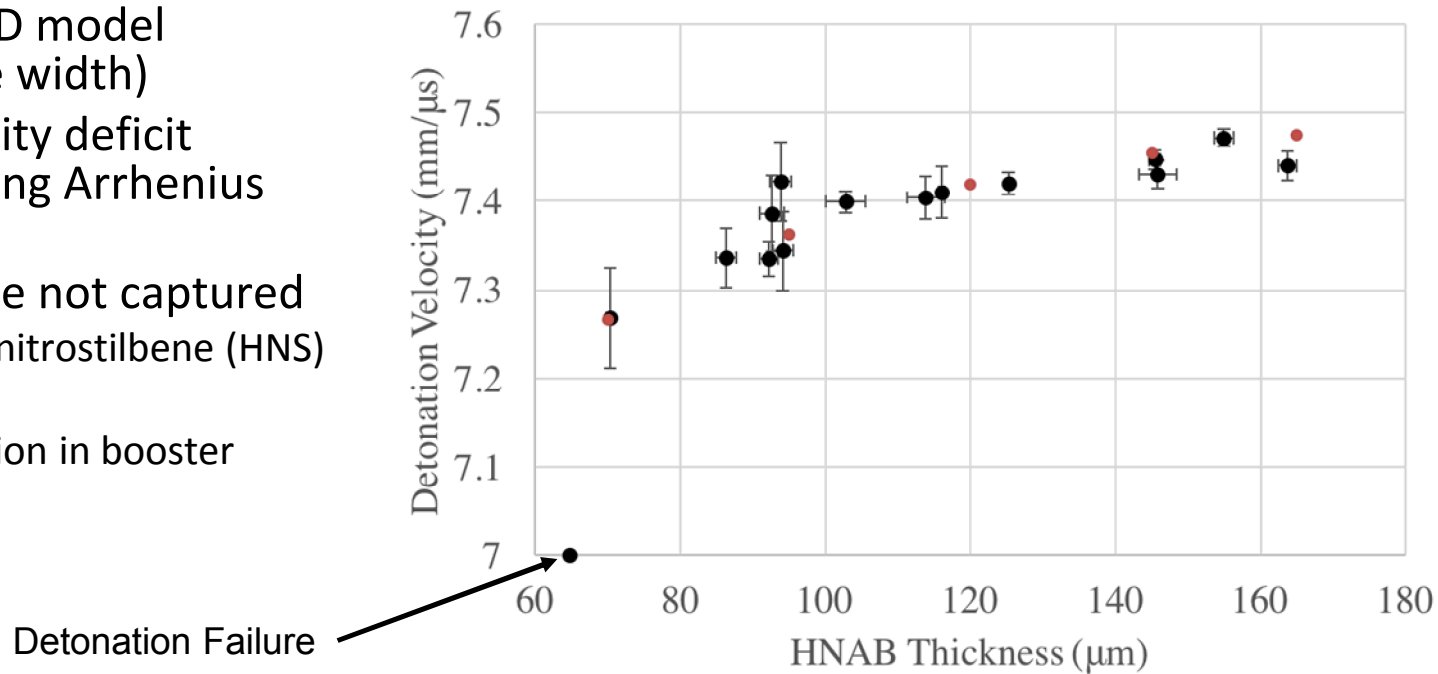
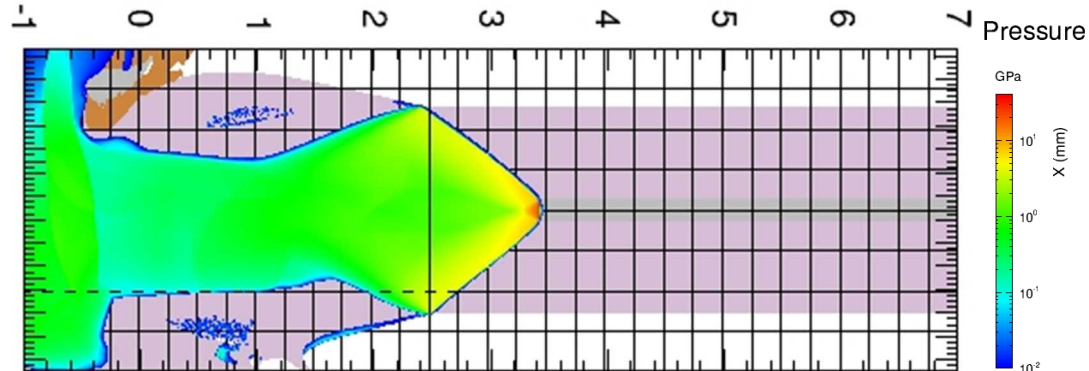
Optical fiber data is used to produce a linear fit to position versus time, where the slope is the velocity.



Photographs of critical detonation thickness experiment. Optical fibers illuminated to highlight position.

Model Fitting and Results

- Density: 1.735 g/cm^3
- Steady roll off in velocity at decreased thicknesses
- Failure to propagate at thickness $< 65 \mu\text{m}$
- Two material PETN model for detonator to match average density
- Cross sectional 2D model (assumed infinite width)
- Detonation velocity deficit captured well using Arrhenius Reactive Burn
- Detonation failure not captured
 - Similar to Hexanitrostilbene (HNS)
 - 3D effects
 - Density resolution in booster



Conclusions

- Amorphous deposited HNAB crystallized at room temperature through gentle abrasive nucleation
- VELOCE crystalline HNAB-II samples prepared through deposition on LiF windows
- Backward integration used to define drive conditions
- HNAB-II EOS and strength parameterization obtained through optimization of continuum model with the VISAR data
- ARB model optimized against experimental velocity vs. thickness data
- Good match to performance data obtained, however further refinement needed to capture failure

Acknowledgements

- Michael P. Marquez, Nicole Cofer, and M. Barry Ritchey
- DICE team
 - Randy Hickman, Keith Hodge, Nicole Cofer, and Joshua Usher
- The Joint Department of Defense/Department of Energy Munitions Technology Development Program
- Laboratory Directed Research and Development

Backup slides

Sample Identifier	HNAB Thickness	HNAB Thickness standard deviation	Window material	Notes
	µm	µm		
SCT928_6	189	1	PMMA	PMMA window #6
SCT951_3	169	4	LiF	LiF window #3

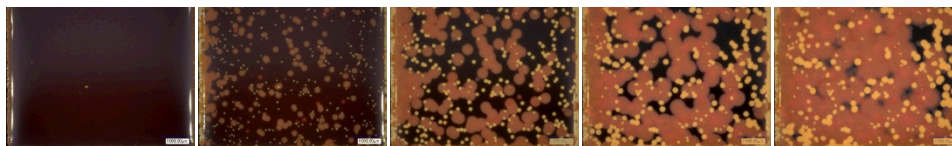
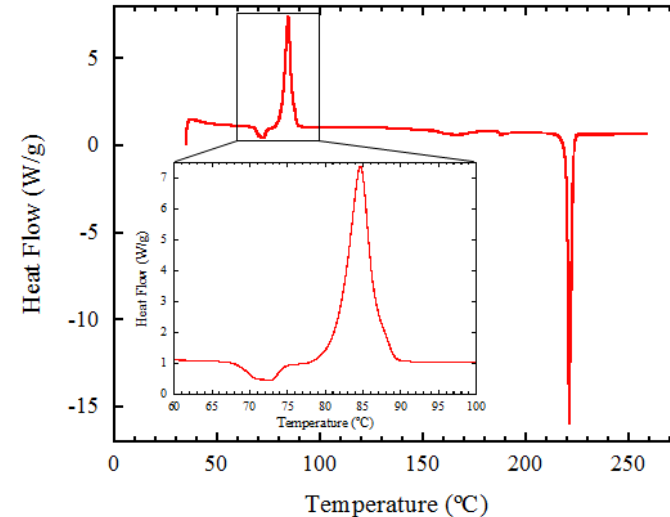
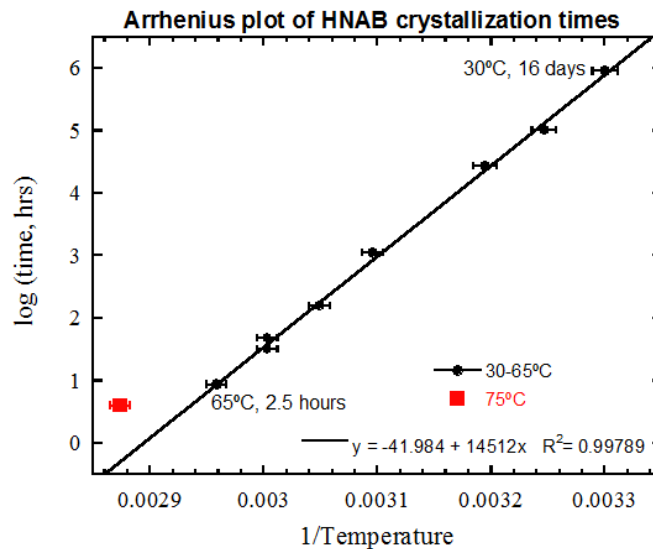
Previous work on vapor deposited HNAB shows that the HNAB crystallizes principally to the HNAB-II polymorph, which has an unstrained crystal density of 1.744 g/cm³.[\[1\]](#) The density of vapor deposited HNAB-II films is estimated to be 99.5% (1.735 g/cm³) from ion-polished cross-section data.[\[2, 3\]](#)

VELOCE samples assembled with Sylgard® 527, low-viscosity silicone.

1. Graeber, E.J. and Morosin, B., "The crystal structures of 2,2',4,4',6,6'-hexanitroazobenzene (HNAB), forms I and II," *Acta Crystallographica Section B*, vol. 30, no. 2, pp. 310-317, 1974.
2. Tappan, A.S., Wixom, R.R., and Knepper, R., "Geometry effects on detonation in vapor-deposited hexanitroazobenzene (HNAB)," *AIP Conference Proceedings*, vol. 1793, no. 1, p. 030036, 2017/01/13, 2015.
3. Knepper, R., unpublished data, Sandia National Laboratories, 2017.

HNAB crystallization

- Amorphous HNAB films crystallize over time
- Pronounced difference in crystallization above glass transition temperature (T_g , ~ 70 °C)



Time-lapse of HNAB crystallization, 65 °C, 24 min./image.

DSC data from an amorphous HNAB film heated from 40–250 °C at 5 °C/min.

Knepper, R., Browning, K., Wixom, R.R., Tappan, A.S., Rodriguez, M.A., and Alam, M.K., "Microstructure Evolution during Crystallization of Vapor-Deposited Hexanitroazobenzene Films," *Propellants, Explosives, Pyrotechnics*, vol. 37, pp. 459 – 467, 2012.